

zfp36 expression delineates both myeloid cells and cells localized to the fusing neural folds in *Xenopus tropicalis*

MAUD NOIRET, SERGE HARDY and YANN AUDIC*

CNRS UMR 6092, Gene Expression and Development Team, Université Rennes 1,
Institut de Génétique et Développement de Rennes (IGDR), Rennes, France

ABSTRACT Regulatory RNA binding proteins allow for specific control of gene expression in a very dynamic manner. In mammals ZFP36, formerly known as Tristetraprolin, controls the inflammatory response by binding to an AU-rich element located in the 3' untranslated region of its target mRNAs. The developing embryo relies on a population of primitive macrophages to ensure proper immunity. Although the role of *zfp36* in adult immunity has been extensively studied, its expression in the developing immune system has been poorly documented. Here, we have used whole mount *in situ* hybridization with a 3' UTR specific probe to address the expression of *zfp36* in developing *Xenopus tropicalis* embryos. We have shown that *zfp36* is expressed in two distinct cellular populations. First, it is a new marker of primitive myeloid cells, being coexpressed with the myeloid marker *mpo*. Therefore this early expression may suggest a role for *zfp36* in macrophage differentiation and activation. In addition, a second cell population was found to transiently express *zfp36*, but not *mpo*, along the fusing neural folds and may correspond to cells undergoing autophagy during neural tube closure.

KEY WORDS: RNA binding proteins, *Xenopus tropicalis*, embryonic immunity

ZFP36 formerly known as Tristetraprolin (TTP) (Lai *et al.*, 2014) belongs to a family of RNA binding Zinc Fingers containing proteins which is composed of 3 members in humans, ZFP36, ZFP36L1 and ZFP36L2. In *Xenopus laevis*, a fourth member previously called C3H4 and named Zfp36L4 has been identified (Belloc and Méndez, 2008; De *et al.*, 1999; Tréguer *et al.*, 2013).

Functionally, ZFP36 has been shown to regulate post-transcriptionally the inflammatory response by controlling the expression level of inflammatory factors such as TNF- α (Carballo *et al.*, 1998) or GM-CSF (Carballo *et al.*, 2000). Mice constitutively deficient for ZFP36, albeit apparently normal at birth develop a debilitating inflammatory response (Taylor *et al.*, 1996). ZFP36 acts through the specific binding to AU-rich element present in the 3'UTR of the targeted mRNAs and triggers their destabilization (Lai *et al.*, 2000).

Extensive work has been conducted to address the function of ZFP36 in the regulation of inflammatory processes while its expression in the developing immune system has been loosely documented. *Xenopus* is a useful model system to study the multiple steps of early immune system development (Ciau-Uitz *et al.*, 2010). In *Xenopus* embryos, primitive hematopoiesis is initiated in a ventral region termed the ventral blood island (VBI) that is the equivalent of the mammalian extraembryonic yolk sac. The

VBI is composed of two areas, the anterior VBI (aVBI) and the posterior VBI (pVBI) that give rise to different cell populations. The aVBI originates from blastomeres C1D1 and comprises an hemangioblast-like population of cells expressing both blood and endothelial cell markers at stage 14. Yet, it has recently been shown that in normal situation the aVBI will only produce blood cells (Myers and Krieg, 2013), the myeloid lineage being highly represented among those. These myeloid cells can be clearly distinguished by following the expression of a peroxidase family member, the myeloperoxidase (*mpo* also known as *xpox2*, (Smith *et al.*, 2002)). *mpo* expression is first detected in the aVBI of early neurula at stage 13 (Tashiro *et al.*, 2006). *mpo*-positive cells undergo proliferation before differentiating and migrating throughout the embryos from stage 19-20. The migrating cells navigate in between the ectodermal and mesodermal layer and in between the mesodermal and endodermal layer. The *mpo*-positive cells are functional myeloid cells that are recruited upon wound healing in *Xenopus* tadpoles (Costa *et al.*, 2008).

Abbreviations used in this paper: aVBI, anterior VBI; ISH, *in situ* hybridization; pVBI, posterior VBI; TTP, Tristetraprolin; VBI, ventral blood island.

*Address correspondence to: Yann Audic. UMR 6290-Génétique et Développement, Faculté de médecine, 2, Avenue du Professeur Léon Bernard, 35043 Rennes Cedex, France. Tel: +33-(0)2-2323-4475. Fax: +33-(0)2-2323-4478. e-mail: yann.audic@univ-rennes1.fr - web: <http://igdr.univ-rennes1.fr>

Accepted: 19 January 2015.

In *Xenopus* as in human the embryonic macrophages are central for the innate immunity of the developing embryos until the adaptive immune system develop later on. They play multiple functions by providing an innate immune function, participating in wound healing (Costa *et al.*, 2008), promoting heart formation (Smith and Mohun, 2011) and in clearing the embryo of apoptotic cells (Hopkinson-Woolley *et al.*, 1994). This last function is particularly important during development since apoptosis is fundamental to many developmental processes (Fuchs and Steller, 2011). In particular, apoptosis is observed during neural tube closure in mice where it is required for proper zipping of the neural ridge (Yamaguchi *et al.*, 2011).

Expression of *zfp36* can be induced rapidly through various stimulation with cytokines, insulin or growth factors (Sanduja *et al.*, 2012). It is also rapidly induced in macrophages following their activation by bacterial pathogens (Nau *et al.*, 2002). A recent study on the ZFP36 family of RNA binding protein in *Xenopus laevis* presented the expression pattern for the 4 members of this family (Tréguer *et al.*, 2013). Particularly, the expression pattern of *zfp36* was presented from stage 24 to stage 34. The authors showed that *zfp36* was detected in somites, cement gland and presented a punctate staining in the lateral mesoderm of the embryos by stages 24, staining that disappeared in later stages embryos. The ontological origine of this staining was not assessed. This prompted us to precise the early *zfp36* expression using the diploid *Xenopus tropicalis*.

Results

Considering that ZFP36 is a protein with a prevalent role in the control of inflammatory process, we hypothesized that the punctate staining observed by Tréguer and colleagues (Tréguer *et al.*, 2013) could be originating from the population of migratory macrophages. To address this hypothesis we first tested whether the published staining pattern was reproducible in *X. tropicalis*.

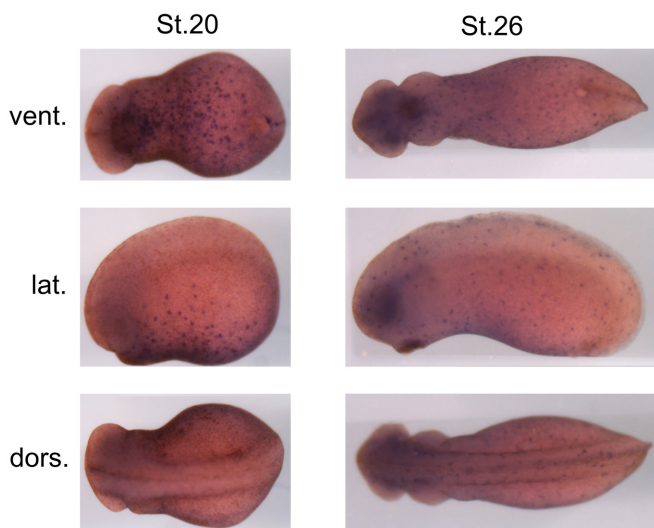


Fig. 1. *In situ* hybridization for *zfp36* using a 3' UTR probe. Stages 20 and 26 *X. tropicalis* embryos were fixed and treated for ISH with a probe targeting the 3' UTR of *zfp36* mRNA. Ventral (vent.), lateral (lat.) and dorsal (dors.) views of representative embryos are shown as indicated.

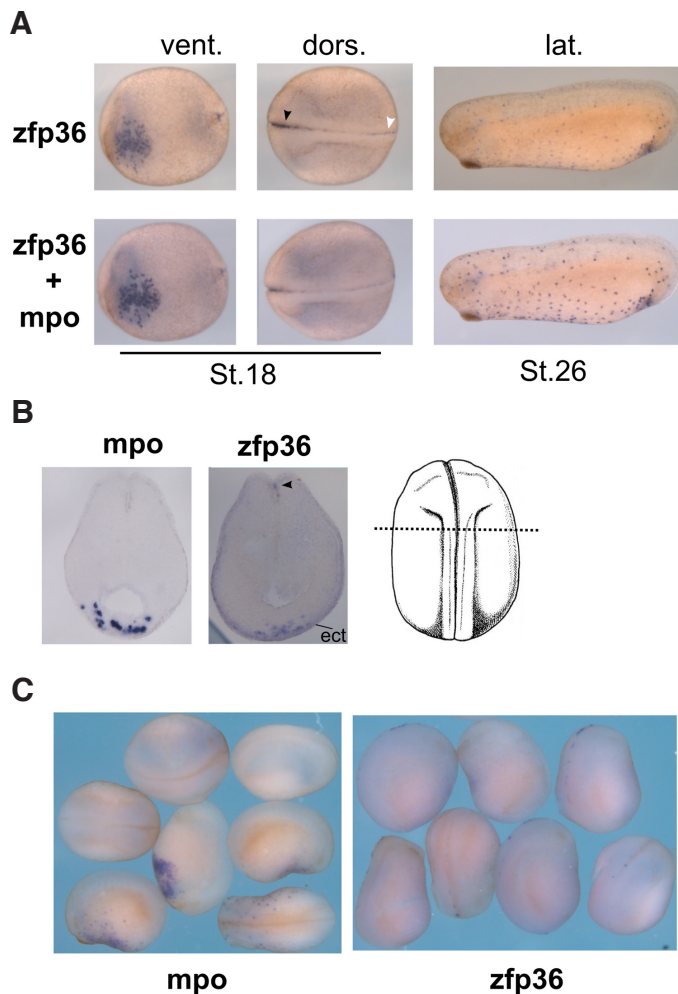


Fig. 2. *zfp36* mRNA is expressed in two different cell populations in early *X. tropicalis* embryos. Double sequential *in situ* hybridization (A) revealed for *zfp36* and *zfp36* + *mpo* in stage 18 and stage 26 embryos. Vibratome section of stage 20 embryos (B) stained for *zfp36* or *mpo* as indicated. The cut plane is shown on the right panel. (C) Mixed view of stages 19-21 embryos stained for *zfp36* or *mpo*. Arrowhead, anterior neural fold staining for *zfp36*, open arrowhead, posterior labeling of neural fold by *zfp36*.

To avoid potential cross-hybridization with the three paralogs, an antisense probe encompassing sequences corresponding to the 3' UTR was used to perform whole mount *in situ* hybridization (ISH) of late neurulae (stage 20) and tailbud embryos (stage 26) (Fig. 1). Consistent with the study of Tréguer and colleagues (Tréguer *et al.*, 2013) a punctate staining was present at both stages. In late neurula (st. 20), this labelling was centered on the ventral region that corresponds likely to the aVBI while at stage 26 the labelled cells extended all over the surface of the embryo. At the tailbud stage a denser area of punctate staining was detected just above the cement gland but this structure itself was not stained. Finally in contrast to the published data no labelling was detected in the somites either at the neurula or tailbud stages (Fig. 1 lateral view).

To determine whether *zfp36* is expressed in cells of the myeloid lineage we conducted sequential double *in situ* hybridization with *zfp36* and *mpo* a specific myeloid marker. *zfp36* and *mpo* specific probes were labeled respectively with digoxigenin and fluores-

cein. Probes were revealed sequentially with anti-DIG/alkaline phosphatase and anti-fluorescein/alkaline phosphatase antibodies using NBT-BCIP as substrate. Phosphatase activity was killed by dehydration in methanol in between immunodetection of each label. As described above, revelation of *zfp36* expression showed that ventrally *zfp36*-positive cells are localized in the anterior part of the embryo in an area compatible with the aVBI. The subsequent detection of *mpo* showed an increase in NBT/BCIP signal in this region of the embryos in the same cells showing that at stage 18 the ventrally *zfp36*-positive cells express *mpo* (Fig. 2A). At stage 26 when the *zfp36*-positive cells have migrated and colonized the whole embryo the coexpression with *mpo* was more clearly observed, each *zfp36*-positive cell being also *mpo*-positive (Figure 2A right panel). To refine the location of *mpo* or *zfp36* expressing cells transversal section of stage 20 embryos stained for *mpo* or *zfp36* were also realized. (Fig. 2B right panel). Both *mpo* and *zfp36* expressing cells were located under the ectoderm in a location where the migration of myeloid cells take place (Fig. 2B). We therefore concluded that *zfp36* is expressed in the primitive myeloid cells that originate from the aVBI and differentiate further into migratory embryonic macrophages.

Interestingly at stage 18 a second cell population expressing *zfp36* was also observed close to the tips of the fusing neural folds with a stronger signal at the anterior and posterior ends (neuropores) (Fig. 2A). These dorsal *zfp36*-positive cells do not present any obvious increase in signal in the sequential double *in situ* hybridization when revealed for *mpo*. In addition, while in transverse sections a few number of *zfp36*-positive cells specifically located along the neural fold could be observed (Fig. 2B middle panel, arrowhead) the *mpo* staining was only detected ventrally (Fig. 2B left panel) suggesting these cells do not correspond to migratory macrophages.

To determine if *mpo* staining could be observed dorsally along the neural fold we conducted single *in situ* hybridization for *mpo* on embryos at stages 19-21. We could never detect any labelling along the neural folds (Fig. 2C, left panel) while *mpo*-positive cells were distinctly detected ventrally. On the contrary, a few *zfp36*-positive cells were clearly detected along the neural folds. Importantly, their number and localization varied from one embryo to the other suggesting they participate in a very dynamic process. This further confirm that *zfp36* labeled at least two different cell populations, a ventral population characterized both by *mpo* and *zfp36* expression and a population of cells expressing only *zfp36* and localized along the fusing neural folds.

To address more precisely the temporal expression pattern of *zfp36* in early embryos we conducted both qRT-PCR and ISH for *zfp36* mRNA during development (Fig. 3). When analyzed by RT-QPCR (Fig. 3A), *zfp36* mRNA was undetected in unfertilized eggs and first detected in stage 10 embryos, accumulating during the neurulation to reach a plateau by stage 23. *zfp36* expression was increased by about 3 fold between stage 12 and stage 23 while *mpo* mRNA levels increased at least 10 fold between stage 16, when it was first detected, and stage 26. The earliest *zfp36* expression we could detect by *in situ* hybridization was at stage 14 in the most anterior part of the ventral mesoderm (Fig. 3B). *zfp36* expression could then be detected ventrally as a spotted pattern in stage 16 embryos. At this stage, no dorsal *zfp36* labeling was present along the neural folds, the blue background being a non-specific staining. The ventral localisation of *zfp36* was further

confirmed in later stages 19 and 21 embryos when *zfp36*-positive cells become more individualized and migrate away from the ventral midline. At stage 24 a distinct salt and pepper pattern covered loosely the whole embryos. At stages 19 and 21, *zfp36*-positive cells were detected along the neural fold where the neural tube closes. Frontal view of stages 19 and 21 embryos allowed the visualization of both ventral and dorsal staining. By stage 24 no *zfp36*-positive cells could be detected dorsally along the neural tube. By stage 32 (Fig. 3C) the punctate staining as vanished but a dense *zfp36* specific staining was observed ventrally close to the heart field. This staining is highly similar to the reported expression of *mpo* at this stage (Smith *et al.*, 2002).

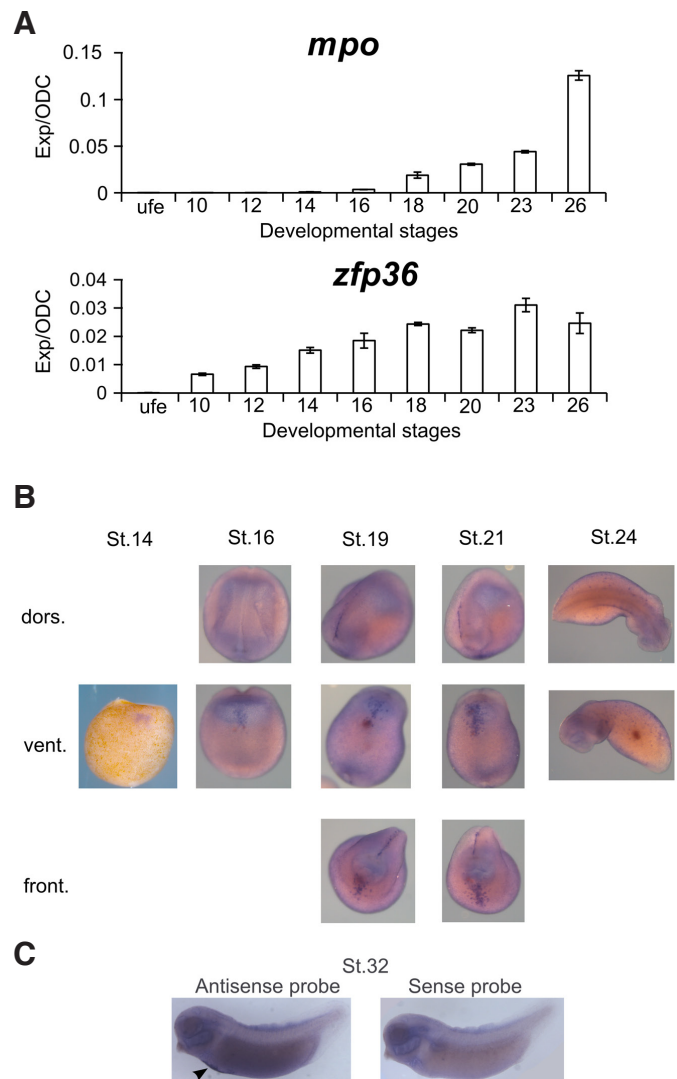


Fig. 3. Spatio-temporal expression of *zfp36* mRNAs in *X. tropicalis* embryos. (A) RT-QPCR on total mRNA for the indicated stages of development for *mpo* and *zfp36* mRNAs. Data are normalized to *odc* mRNAs. (B) Stage 14 to stage 24 *X. tropicalis* embryos are stained for *zfp36* mRNAs and pictured from dorsal, ventral or frontal views. *zfp36* mRNA is localized in the aVBI from stage 14 and along the neural fold starting from stage 19. (C) Stage 32 *X. tropicalis* embryos are stained for *zfp36* mRNA with a sense or antisense probe as indicated. The dense ventral staining is indicated by an arrowhead.

Discussion

Our data showed that *zfp36* is first expressed around stage 14 in the antero-ventral part of the embryo in an area corresponding to the aVBI. Lately, the expression spread to cover the whole embryo in a spotted pattern by the late tailbud stage. Double *in situ* hybridizations with *mpo*, a marker of the myeloid cell lineage has revealed that these cells correspond to population of migratory macrophages that move under the ectoderm and define therefore *zfp36* as a new marker of the embryonic myeloid lineage. Such an expression of *zfp36* in primitive myeloid cells originating from the aVBI in *Xenopus* is in agreement with its expression in the adult myeloid lineage in mammals. In adult macrophages ZFP36 destabilizes pro-inflammatory transcripts among which TNF-alpha by binding to the AU-rich element of its 3' untranslated region (Reviewed in (Sanduja et al., 2012)). This inactivation by ZFP36 is central in an autoregulatory feedback loop that limits the inflammatory response. The *X. tropicalis* TNF 3'UTR being also highly rich in AU-rich element suggests a conservation of the process at play. Yet nothing is known on the role of *Zfp36* in the establishment of the primitive myeloid lineage.

We could not detect any expression in the dorsal lateral plate at any stages of development ruling out an early expression of *zfp36* in a domain that will give rise to adult blood cells.

In contradiction to what has been previously reported in *X. laevis*, no expression of *zfp36* in the somites and the cement gland was observed in *X. tropicalis*. These differences may originate from cross-hybridization of the full length probe used in the former study with the other paralogs. Alternatively in *X. laevis* the duplicated *zfp36* genes may display different expression patterns. Interestingly, comparative transcriptomic analysis of *X. laevis* and *X. tropicalis* gene expression highlighted divergence in the temporal expression of genes involved in innate immunity (Yanai et al., 2011). These temporal divergence could be accompanied by divergence in the spatial expression as we observe here for *zfp36*.

Importantly, between stage 19 and stage 22, *zfp36* is also expressed in a few number of cells specifically located at the extremity of the fusing neural folds. Their number and localization vary from one embryo to the other and they do not express *mpo*. This therefore raises two important questions:

Origin of *zfp36*-positive cells and function in the fusing neural fold

Data from the literature do not show any specific expression of hematopoietic genes along the neural folds in stages when *zfp36* is expressed (Chen et al., 2009). In addition, it is unlikely that these *zfp36*-positive cells migrate from the aVBI as the migration of the myeloid cells has just started when *zfp36* neuropore staining is first observed, indicating they are not migratory macrophages. This suggests that *zfp36*-positive *mpo*-negative cells located along the neural fold are not originating from the aVBI and define therefore a distinct subpopulation of specialized cells. Furthermore the expression of *zfp36* in these cells is very transitory as later stage embryos do not present *zfp36* staining along the neural tube suggesting they participate in a very dynamic process. In *Xenopus*, the expression pattern of *beclin1*, at stage 19 is partially similar to the expression of *zfp36* with a distinctive speckled pattern along the neural fold (Bowes et al., 2010). Beclin-1 is involved in the activation of the autophagy pathway a process which is accom-

panied by an increase in ERK signaling (Florkowska et al., 2012; Martinez-Lopez et al., 2013). Because neural tube closure appears as being critically controlled by autophagy and apoptosis (Cecconi et al., 2008) it is therefore possible that *zfp36* labelling along the neural folds represent a transient activation of *zfp36* expression in cells undergoing apoptosis or autophagy.

In conclusion, we have shown that *zfp36* is a new marker of primitive myeloid cells whose early expression is compatible with a role in macrophage differentiation and activation. In addition, a second cell population express transiently *zfp36* along the fusing neural folds and may correspond to cells undergoing autophagy during the neural tube closure. To study further the functions of ZFP36 in both cell lineages it will be of interest to use functional approaches including loss of function experiments.

Material and Methods

Xenopus tropicalis in vitro fertilization

X. tropicalis female were primed with 15U hCG (Organon) the day before fertilization experiment. Fourteen hours later female were induced to lay eggs by injection of 100U hCG. Testis were dissected from a *X. tropicalis* male and dilacerated in 300 µl of L15 medium complemented with 10% FBS. Eggs freshly collected from the females were covered with the testis suspension for 3 min and overlaid with water from the aquarium. After 20 min, eggs were dejellied in 2% cysteine in 1X F1 (Hepes 10 mM, NaHCO₃ 2 mM, CaCl₂ 0.25 mM, MgCl₂ 0.6 mM, NaCl 31 mM, KCl 1.75 mM) at pH 7.9, rinsed in 1X F1. Dejjellied embryos were allowed to develop at 22°C on plastic petri dishes covered with 1% agar in water. Embryos were transferred to 0.1X F1 five hours after fertilization. At the chosen time of development, embryos were fixed for 2 hours in freshly prepared MEMFA (0.1 M MOPS pH 7.4, 2 mM EGTA, 1 mM MgSO₄, 3.7% formaldehyde) rinsed in PBS and stored in MeOH at -20°C.

Clones, templates and probe preparation

Plasmids containing the full length cDNA for *mpo* (BQ522393, IMAGEID 5336501) and *zfp36* (BC154918, IMAGEID 8911341) were obtained from Source BioScience. Templates for *in vitro* transcription were as follow: *zfp36*, 3' UTR, antisense probe, *NheI*, T7; *zfp36*, 3' UTR, antisense probe, *NheI*, SP6. *mpo*, full length, sense probe, *XbaI*, SP6; *mpo*, full length, antisense probe, *EcoRI*, T7.

Full length or 3' UTR digoxigenin (Roche) or fluorescein (PerkinElmer) labeled antisense and sense probe were generated by *in vitro* transcription using either T7 or SP6 RNA polymerase (Promega) as indicated above.

In situ hybridization, vibratome sectioning

Whole mount *in situ* hybridization were realized essentially as described in (Harland, 1991). Detection was carried out using anti-DIG or anti-fluorescein Alkaline Phosphatase conjugated antibodies (Roche) and stained with NBT/BCIP (Promega) as substrate. Embryos were bleached in 1.2% hydrogen peroxide in SSC. For detailed analysis embryos treated for whole mount *in situ* hybridization and stored in PBST were embedded in 5% agar and sectioned on a LEICA VT 1200S vibratome at 50 µm thickness as described in (Noiret et al., 2012). Pictures were taken on a Leica Z16 APO microscope.

RNA extraction and RT-QPCR

Total RNA was extracted from pool of 10 *Xenopus tropicalis* embryos at the indicated stages (Nieuwkoop and Faber, 1994) using Tri-reagent following manufacturer recommendations (Molecular Research center). Genomic contamination was eliminated by treatment with TurboTM Dnase (Ambion) Total RNA was reverse transcribed using random primers and Superscript II reverse transcriptase (Invitrogen). QPCR was performed on a qPCR7900 HT (Applied Biosystems) using the Sybr Green Master mix (Life Technologies) with the following oligonucleotides pairs: *odc* (Noiret et al.,

2012), *mpo* (Costa *et al.*, 2008), *zfp36_forward* caaacgcacccaaagtataa, *zfp36_reverse* tgcttgccacaccagaatg. QPCR results were normalized to *odc* levels.

Acknowledgement

The authors acknowledge the contribution of Mr Gerard Fenech and Sylvain Pastezeur for animal care and the H2P2 platform of Biosit (UMS CNRS 3480 / US INSERM 018) for histological analysis. Maud Noiret was supported by a Ph.D fellowship from the Ministère de l'éducation nationale, de l'enseignement supérieur et de la recherche. We are grateful to Nicolas Pollet for insightful discussion.

References

- BELLOC E, MÉNDEZ R (2008). A deadenylation negative feedback mechanism governs meiotic metaphase arrest. *Nature* 452: 1017-1021.
- BOWES JB, SNYDER KA, SEGERDELL E, JARABEK CJ, AZAM K, ZORN AM, VIZE PD (2010). Xenbase: gene expression and improved integration. *Nucleic Acids Res* 38: D607-612.
- CARBALLO E, LAI WS, BLACKSHEAR PJ (2000). Evidence that tristetraprolin is a physiological regulator of granulocyte-macrophage colony-stimulating factor messenger RNA deadenylation and stability. *Blood* 95: 1891-1899.
- CARBALLO E, LAI WS, BLACKSHEAR PJ (1998). Feedback inhibition of macrophage tumor necrosis factor- α production by tristetraprolin. *Science* 281: 1001-1005.
- CECCONI F, PIACENTINI M, FIMIA GM (2008). The involvement of cell death and survival in neural tube defects: a distinct role for apoptosis and autophagy? *Cell Death Differ* 15: 1170-1177.
- CHEN Y, COSTA RMB, LOVE NR, SOTO X, ROTH M, PAREDES R, AMAYA E (2009). C/EBP α initiates primitive myelopoiesis in pluripotent embryonic cells. *Blood* 114: 40-48.
- CIAU-UITZ A, LIU F, PATIENT R (2010). Genetic control of hematopoietic development in *Xenopus* and zebrafish. *Int J Dev Biol* 54: 1139-1149.
- COSTA RMB, SOTO X, CHEN Y, ZORN AM, AMAYA E (2008). spib is required for primitive myeloid development in *Xenopus*. *Blood* 112: 2287-2296.
- DE J, LAI WS, THORN JM, GOLDSWORTHY SM, LIU X, BLACKWELL TK, BLACKSHEAR PJ (1999). Identification of four CCCH zinc finger proteins in *Xenopus*, including a novel vertebrate protein with four zinc fingers and severely restricted expression. *Gene* 228: 133-145.
- FLORKOWSKA M, TYMOSZUK P, BALWIERZA, SKUCHAA, KOCHAN J, WAWRO M, STALINSKA K, KASZAA (2012). EGF activates TTP expression by activation of ELK-1 and EGR-1 transcription factors. *BMC Mol Biol* 13: 8.
- FUCHS Y, STELLER H (2011). Programmed cell death in animal development and disease. *Cell* 147: 742-758.
- HARLAND RM (1991). *In situ* hybridization: an improved whole-mount method for *Xenopus* embryos. *Methods Cell Biol* 36: 685-695.
- HOPKINSON-WOOLLEY J, HUGHES D, GORDON S, MARTIN P (1994). Macrophage recruitment during limb development and wound healing in the embryonic and foetal mouse. *J Cell Sci* 107 (Pt 5): 1159-1167.
- LAI WS, CARBALLO E, THORN JM, KENNINGTON EA, BLACKSHEAR PJ (2000). Interactions of CCCH zinc finger proteins with mRNA. Binding of tristetraprolin-related zinc finger proteins to Au-rich elements and destabilization of mRNA. *J Biol Chem* 275: 17827-17837.
- LAI WS, PERERA L, HICKS SN, BLACKSHEAR PJ (2014). Mutational and structural analysis of the tandem zinc finger domain of tristetraprolin. *J Biol Chem* 289: 565-580.
- MARTINEZ-LOPEZ N, ATHONVARANGKUL D, MISHALL P, SAHU S, SINGH R (2013). Autophagy proteins regulate ERK phosphorylation. *Nat Commun* 4: 2799.
- MYERS CT, KRIEG PA (2013). BMP-mediated specification of the erythroid lineage suppresses endothelial development in blood island precursors. *Blood* 122: 3929-3939.
- NAU GJ, RICHMOND JFL, SCHLESINGERA, JENNINGS EG, LANDERES, YOUNG RA (2002). Human macrophage activation programs induced by bacterial pathogens. *Proc Natl Acad Sci USA* 99: 1503-1508.
- NIEUWKOOP PD, FABER J (1994). *Normal Table of Xenopus laevis (Daudin): A Systematical and Chronological Survey of the Development from the Fertilized Egg Till the End of Metamorphosis*. Garland Pub.
- NOIRET M, AUDIC Y, HARDY S (2012). Expression analysis of the polypyrimidine tract binding protein (PTBP1) and its paralogs PTBP2 and PTBP3 during *Xenopus tropicalis* embryogenesis. *Int J Dev Biol* 56: 747-753.
- SANDUJA S, BLANCO FF, YOUNG LE, KAZA V, DIXON DA (2012). The role of tristetraprolin in cancer and inflammation. *Front Biosci* 17: 174-188.
- SMITH SJ, KOTECHEA S, TOWERS N, LATINKIC BV, MOHUN TJ (2002). XPOX2-peroxidase expression and the XLURP-1 promoter reveal the site of embryonic myeloid cell development in *Xenopus*. *Mech Dev* 117: 173-186.
- SMITH SJ, MOHUN TJ (2011). Early cardiac morphogenesis defects caused by loss of embryonic macrophage function in *Xenopus*. *Mech Dev* 128: 303-315.
- TASHIRO S, SEDOHARA A, ASASHIMA M, IZUTSU Y, MAÉNO M (2006). Characterization of myeloid cells derived from the anterior ventral mesoderm in the *Xenopus laevis* embryo. *Dev Growth Differ* 48: 499-512.
- TAYLOR GA, CARBALLO E, LEE DM, LAI WS, THOMPSON MJ, PATEL DD, SCHENKMAN DI, GILKESON GS, BROXMEYER HE, HAYNES BF, BLACKSHEAR PJ (1996). A pathogenetic role for TNF α in the syndrome of cachexia, arthritis, and autoimmunity resulting from tristetraprolin (TTP) deficiency. *Immunity* 4: 445-454.
- TRÉGUER K, FAUCHEUX C, VESCHAMBRE P, FÉDOU S, THÉZÉ N, THIÉBAUD P (2013). Comparative functional analysis of ZFP36 genes during *Xenopus* development. *PLoS ONE* 8: e54550.
- YAMAGUCHI Y, SHINOTSUKA N, NONOMURA K, TAKEMOTO K, KUIDA K, YOSIDA H, MIURAM (2011). Live imaging of apoptosis in a novel transgenic mouse highlights its role in neural tube closure. *J Cell Biol* 195: 1047-1060.
- YANAI I, PESHKIN L, JORGENSEN P, KIRSCHNER MW (2011). Mapping gene expression in two *Xenopus* species: evolutionary constraints and developmental flexibility. *Dev Cell* 20: 483-496.

Further Related Reading, published previously in the *Int. J. Dev. Biol.*

Hippo signaling components, Mst1 and Mst2, act as a switch between self-renewal and differentiation in *Xenopus* hematopoietic and endothelial progenitors

Susumu Nejigane, Shuji Takahashi, Yoshikazu Haramoto, Tatsuo Michiue and Makoto Asashima
Int. J. Dev. Biol. 57: 407 - 414 (2013)

Differential expression of the Bruno/CELF family genes during *Xenopus laevis* early development

Jingyang Wu1, Chaocui Li1, Shuhua Zhao and Bingyu Mao
Int. J. Dev. Biol. 54: 209 - 214 (2010)

Gene regulatory networks governing haematopoietic stem cell development and identity

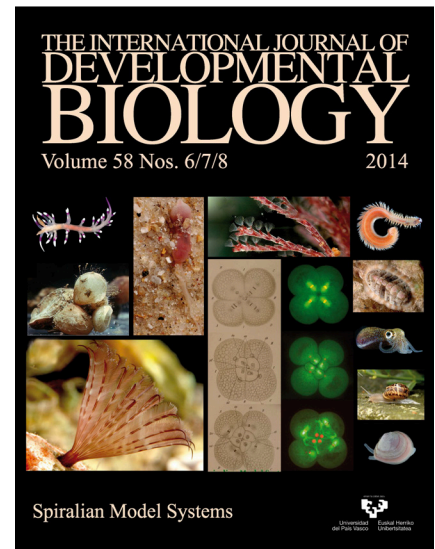
John E. Pimanda and Berthold Göttgens
Int. J. Dev. Biol. 54: 1201 - 1211 (2010)

Expression of complement components coincides with early patterning and organogenesis in *Xenopus laevis*

Valérie A. McLin, Cheng-Hui Hu, Rina Shah and Milan Jamrich
Int. J. Dev. Biol. 52: 1123 - 1133 (2008)

Developmental biology of zebrafish myeloid cells

Meredith O Crowhurst, Judith E Layton and Graham J Lieschke
Int. J. Dev. Biol. 46: 483 - 492 (2002)



5 yr ISI Impact Factor (2013) = 2.879

